Progress In Electromagnetics Research, Vol. 154, 163–170, 2015

Quantum Mechanical Modeling of Electron-Photon Interactions in Nanoscale Devices

Rulin Wang[1], Yu Zhang[2], Guanhua Chen[2], and Chiyung Yam[1, 2, *]

(*Invited Paper*)

Abstract—An efficient quantum mechanical approach is formulated to model electron-photon interactions in nanoscale devices. Based on nonequilibrium Green's function formalism, electron-photon interactions and open boundaries in the nanoscale systems are taken into account in terms of self-energies. By separating different components in the electron-photon interactions, optical absorption and emission processes in the devices can be analyzed, and the method allows studies of different optoelectronic devices. In conjunction with density-functional tight-binding method, photo-induced current and other optical properties of nanoscale devices can be simulated without relying on empirical parameters. To demonstrate our approach, numerical studies of gallium nitride nanowire solar cells of realistic sizes are presented.

1. INTRODUCTION

Optoelectronics has become an important part of our lives, which encompasses the application of electronic devices to convert electrical signals into optical signals and vice versa. The most common and long studied example, photovoltaics, converts solar energy to electrical energy and is playing a key role in the development of future renewable energy resources. Other applications include light-emitting diodes, sensing systems, fiber optic communications, lasers, medical diagnostic systems and optical information systems. Owing to the continuous advancements in lithographic resolution, modern technology allows fabrication of optoelectronic devices with nanoscale semiconductor structures. These devices take advantage of sophisticated interactions between electrons and light. In this context, light is not limited to visible region of the electromagnetic spectrum but includes also invisible forms of radiation. While developments in the semiconductor industry have relied on the continued scaling down of size of electronic and optoelectronic devices, their shrinking size and increasing complexity make fabrications and measurements of nanoscale devices extremely expensive and time-consuming.

Given the complexity of modern nanoscale devices, computer simulation becomes an indispensable tool for both understanding the properties of existing devices and designing next generation devices that meet ever increasing performance demands. Theoretical methods based on classical models [1, 2] have been developed to describe interaction with light in electronic devices. They, however, rely on empirical parameters and fail to describe quantum effect. As the size of modern electronic and optoelectronic devices continues to scale down, microscopic approaches based on atomistic simulations are inevitable to account for the quantum mechanical phenomena that affect both transport and optical properties of nanoscale devices. It is thus desirable to develop a quantum mechanical microscopic quantum theory for the description of nanoscale optoelectronic devices. While interactions between electrons

Received 29 November 2015, Accepted 21 December 2015, Scheduled 31 December 2015
Invited paper for the Commemorative Collection on the 150-Year Anniversary of Maxwell's Equations.
* Corresponding author: Chiyung Yam (yamcy@csrc.ac.cn).
[1] Beijing Computational Science Research Center, Beijing 100094, China. [2] Department of Chemistry, The University of Hong Kong, Hong Kong, China.

and light have been a standard problem in the context of spectroscopy, their theoretical description in optoelectronic devices is much challenging. The reason for this is twofold. First, the devices are open systems in contact with electron reservoirs which are subjected to an external bias voltage. In addition to the electron flux caused by external bias, the devices are driven out of equilibrium by the incident electromagnetic radiation. It is thus necessary to describe systems which are in non-equilibrium state. Second, inter-related processes in which devices emit light in response to the passage of an electric current or photoassisted electron transport are necessary to account for. Thus, optical and electronic properties of the nanoscale structures need to be described with high accuracy.

Quantum transport approach based on nonequilibrium Green's function (NEGF) method has been widely used to study electrical properties of electronic devices [3–8]. Taking into account electron-photon interactions, the approach provides an efficient and versatile way to describe the coupled optical electrical processes in nanoscale devices [9–12]. By imposing open boundary conditions, the formalism allows treatment of both coherent and incoherent transport of devices in contact with electron reservoirs characterized by different chemical potentials. The NEGF method provides information on the electronic states together with their population statistics. Incoherent transport can be described by introducing appropriate self-energy terms which can be derived systematically from many-body perturbation theory [13]. By including electron-photon and electron-phonon interactions, inelastic scattering processes where electrons move among different energy levels can be treated in principle exactly. Thus, this can be applied to simulate process including photo-excitation, electron-hole recombination, charge carrier migration, and heat dissipation in nanoscale devices without resorting to any classical or semi-classical approximations. For optoelectronics, photo-induced current and current-induced light emission in realistic nanoscale devices can be treated within a simple unified framework. In this work, we present our recent implementation of density-functional tight-binding (DFTB)-based NEGF method for modeling interaction of nanoscale devices with light [12–15]. Following its introduction in Section 2, the method is applied to study the performance of realistic nanowire-based photovoltaic devices and numerical results are presented in Section 3.

2. METHODOLOGY

To describe photoexcited processes in devices using quantum transport equations, the interaction Hamiltonian and self-energies for the electron-photon interaction have to be first defined [9]. We start with the full Hamiltonian which includes the electromagnetic interactions

$$H = \frac{1}{2m}\left(\vec{p} + e\vec{A}\right)^2 + V \tag{1}$$

where $\vec{A}$ represents the time-dependent electromagnetic vector potential, V the scalar potential, $\vec{p}$ the electronic momentum operator, e the elementary charge and m the electron mass. Neglecting the nonlinear term in the electromagnetic vector potential, the Hamiltonian is separated into a zeroth-order term and an electromagnetic interaction term,

$$H = H^{\mathrm{el}} + H^{\mathrm{ep}} = \frac{\vec{p}^2}{2m} + V + \frac{e}{m}\vec{A}\cdot\vec{p} \tag{2}$$

where H^{el} is the electronic Hamiltonian described at DFTB level [16, 17]. The last term in the above equation gives the interaction Hamiltonian which is the basis for the electron-photon interaction self-energy. Considering plane wave electromagnetic field with homogeneous susceptibility and dielectric constants, the electromagnetic vector potential and interaction Hamiltonian are given by,

$$\begin{aligned}\vec{A}(t) &= \sum_q \vec{a}_q\left(\frac{\hbar\sqrt{\tilde{\mu}\tilde{\epsilon}}}{2N_q\omega_q\epsilon c}I_q\right)^{1/2}\left(b_q e^{-i\omega_q t} + b_q^\dagger e^{i\omega_q t}\right),\\ H^{\mathrm{ep}} &= \sum_{ij}\sum_q M_{q,ij}\left(b_q e^{-i\omega_q t} + b_q^\dagger e^{i\omega_q t}\right)d_i^\dagger d_j,\end{aligned} \tag{3}$$

respectively. Here, $\tilde{\mu}$ and $\tilde{\epsilon}$ are relative magnetic and dielectric constants, respectively. ϵ is the dielectric constant, $\hbar$ the reduced Planck constant, c the light speed, and q the photon mode characterized by

its frequency ω_q, polarization direction vector $\vec{a}_q$ and occupation number N_q. I_q is photon flux, defined as the number of incident photons per unit time per unit area. b_q and $b_q^\dagger$ are the annihilation and creation operators of photon mode q, respectively. d and $d^\dagger$ are the annihilation and creation operators of electron. M_q is defined as electron-photon coupling matrix for electromagnetic mode q

$$M_{q,ij} = e\left(\frac{\hbar\sqrt{\tilde{\mu}\tilde{\epsilon}}}{2N_q\omega_q\epsilon c} I_q\right)^{1/2} \vec{a}_q \cdot \left\langle i \left| \frac{\vec{p}}{m} \right| j \right\rangle. \tag{4}$$

Using many-body perturbation theory [13], the self-energies for electron-photon interaction at the lowest order are given by

$$\Sigma_{\text{ep}}^{<,>}(t_1,t_2) = i\sum_q M_q G^{<,>}(t_1,t_2) D_q^{<,>}(t_1,t_2) M_q \tag{5}$$

where $G^{<,>}$ are lesser and greater self-energies, giving respectively population statistics of electron and hole densities. Applying commutation relations for the bosonic annihilation and creation operators,

$$\begin{aligned}\langle b_q(t_1) b_q^\dagger(t_2)\rangle &= (N_q+1)e^{-i\omega_q(t_1-t_2)} \\ \langle b_q^\dagger(t_1) b_q(t_2)\rangle &= N_q e^{i\omega_q(t_1-t_2)}\end{aligned} \tag{6}$$

the photon Green's functions, $D_q^{<,>}$, are given by

$$D_q^{<,>}(t_1,t_2) = -i\left[N_q e^{\mp i\omega_q(t_1-t_2)} + (N_q+1)e^{\pm i\omega_q(t_1-t_2)}\right] \tag{7}$$

Substituting Eq. (7) into Eq. (5), electron-photon interaction self-energy in energy domain can be obtained by Fourier transformation with respect to $t_1 - t_2$

$$\Sigma_{\text{ep}}^{<,>}(E) = \sum_q M_q\left[N_q G^{<,>}(E\mp\hbar\omega_q) + (N_q+1)G^{<,>}(E\pm\hbar\omega_q)\right] M_q \tag{8}$$

$G^{<,>}$ can be obtained from Keldysh equation [3],

$$G^{<,>}(E) = G^r(E)\Sigma^{<,>}(E)G^a(E). \tag{9}$$

where G^r and G^a are the retarded and advanced Green's functions, respectively. $\Sigma^{<,>}$ includes all scattering processes from contacts and electron-photon interactions,

$$\Sigma^{<,>}(E) = \sum_\alpha \Sigma_\alpha^{<,>}(E) + \Sigma_{\text{ep}}^{<,>}(E) \tag{10}$$

where $\Sigma_\alpha^{<,>}$ are the self-energies for the α contact. In this work, we consider weak electron-photon interactions where the influence of the interactions on Green's functions can be neglected. Thus, the bare Green's function $G_0(E)$ is used for construction of $\Sigma_{\text{ep}}^{<,>}$

$$\Sigma_{\text{ep}}^{<,>}(E) = \sum_q M_q\left[N_q G_0^{<,>}(E\mp\hbar\omega_q) + (N_q+1)G_0^{<,>}(E\pm\hbar\omega_q)\right] M_q \tag{11}$$

and

$$G_0^{<,>}(E) = \sum_\alpha G_0^r(E)\Sigma_\alpha^{<,>}(E)G_0^a(E). \tag{12}$$

where G_0^r and G_0^a are Green's functions giving the electron structure of the system without influence of electron-photon interactions. The steady state current through the system is computed using the Meir-Wingreen formula [4,5]

$$I_\alpha = \frac{2e}{\hbar}\int\frac{dE}{2\pi}\text{Tr}\left[\Sigma_\alpha^<(E)G^>(E) - \Sigma_\alpha^>(E)G^<(E)\right] \tag{13}$$

The first term of Eq. (13) can be interpreted as the outgoing of electrons from system through contact α while the second term is the incoming rate of electrons to the system from contact α. Substituting

Eq. (9) into Eq. (13), the steady state current I_α can be divided into two terms [12],

$$\begin{aligned} I_\alpha &= I_\alpha^{\text{elastic}} + I_\alpha^{\text{inelastic}} \\ I_\alpha^{\text{elastic}} &= \frac{2e}{\hbar}\sum_{\beta\neq\alpha}\int\frac{dE}{2\pi}[f_\alpha(E)-f_\beta(E)]T(E) \\ I_\alpha^{\text{inelastic}} &= \frac{2e}{\hbar}\int\frac{dE}{2\pi}\text{Tr}\left\{\Gamma_\alpha(E)G_0^r(E)\Gamma_{\text{eff}}(E)G_0^a(E)\right\}, \end{aligned} \tag{14}$$

where

$$\Gamma_{\mathit{eff}}(E) = i\left\{f_\alpha(E)\Sigma_{\text{ep}}^{>}(E) - [f_\alpha(E)-1]\Sigma_{\text{ep}}^{<}(E)\right\} \tag{15}$$

and $T(E)$ is the transmission coefficients, $f(E)$ the Fermi-Dirac distribution function, $I_\alpha^{\text{elastic}}$ the current for non-interacting systems obtained from standard Landauer-Büttiker formula, and $I_\alpha^{\text{inelastic}}$ the inelastic part contributing from the electron-photon interactions. Similarly, the absorption and emission flux of the system for individual electromagnetic mode q can be determined by replacing $\Sigma_\alpha^{<,>}$ in Eq. (13) by their contributions to $\Sigma_{\text{ep}}^{<,>}$,

$$F^{\text{abs}}(\omega_q) = \frac{2}{\hbar}\int\frac{dE}{2\pi}\text{Tr}N_q\left[M_qG_0^{>}(E)M_qG_0^{<}(E-\hbar\omega_q)\right] \tag{16}$$

$$F^{\text{em}}(\omega_q) = \frac{2}{\hbar}\int\frac{dE}{2\pi}\text{Tr}(N_q+1)\left[M_qG_0^{>}(E)M_qG_0^{<}(E+\hbar\omega_q)\right] \tag{17}$$

Here, $F^{\text{abs}}(\omega_q)$ represents an excitation of electron from energy level $E-\hbar\omega_q$ to E, corresponding to an absorption process while $F^{\text{em}}(\omega_q)$ gives the reverse transition from $E+\hbar\omega_q$ to E, which corresponds to the stimulated emission process. For spontaneous emission, the photon occupation number is zero, and the emission flux is given by

$$F^{\text{em}}(\omega_q) = \frac{2}{\hbar}\int\frac{dE}{2\pi}\text{Tr}\left[M_qG_0^{>}(E)M_qG_0^{<}(E+\hbar\omega_q)\right] \tag{18}$$

3. NUMERICAL RESULTS

Gallium nitride (GaN) is an important wide and direct bandgap semiconductor which finds its applications in various optoelectronics [18–20]. Due to the quantum confinement effects, nanostructured devices have attracted extensive research interests for their enhanced electronic and optical properties. Recent studies report that nanowire-based solar cells are able to achieve high power conversion efficiency (PCE) [21, 22]. In this work, we apply the method described in Section 2 to simulate the performance of GaN nanowire solar cells. Wurtzite GaN nanowire oriented in the [0001] direction is investigated with cross section diameter of 1.6 nm and length of 10 nm. To eliminate impact of the surface dangling bonds, the nanowire is passivated with hydrogen atoms. The atomistic model for the device part employed in this work contains 2880 atoms in total, and the cross section is shown in Fig. 1(a). To form a p-n junction, virtual crystal approximation (VCA) [23] is adopted where positive charges are given to gallium atoms on the left region of the nanowire and negative charges given to nitrogen atoms on the right region. The doping concentration is set as $1.0\times10^{20}\,\text{cm}^{-3}$. In the simulations, the nanowire is considered as an open system connected to two semi-infinite leads. The leads have the same doping concentration, characterized by different chemical potentials. The electronic structure of the model is described at DFTB level. All simulations are performed at 300 K with incident light power fixed at $1\,\text{kW/m}^2$.

Figures 1(b) and (c) show the band structures of p-doped and n-doped GaN nanowires, respectively. Examining the states at valence band edge, the orbital contributions are mainly from the $2p$ orbitals on the nitrogen atoms, while the conduction band is narrow with contributions mainly from $4p$ orbitals on the gallium atoms. The calculated bandgap is 3.21 eV. Upon connection of p-doped and n-doped nanowire, charge carriers at the interface will reshuffle and form a space charge region. The valence and conduction bands in the space charge region are bent. With VCA, Fermi levels lie at the VBM of p-doped nanowire and CBM of n-doped nanowire as shown in Fig. 1. Thus, a built-in voltage V_{bi} of 3.20 V

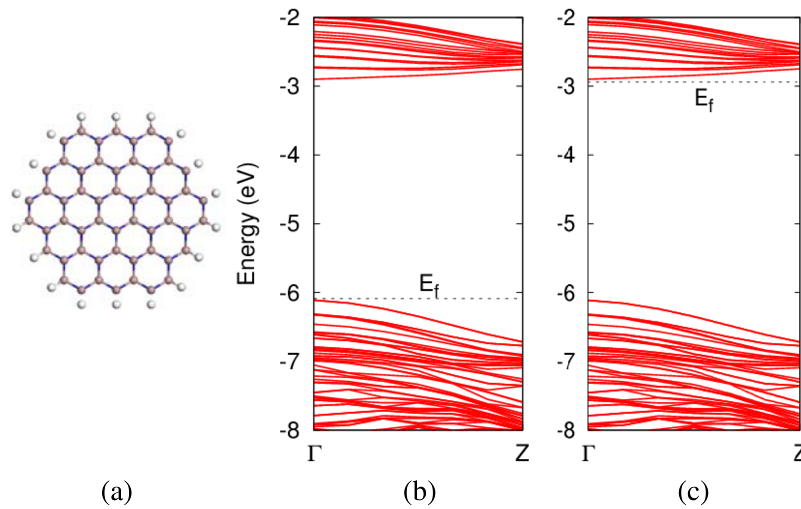

Figure 1. (a) Cross section of a 10 nm long GaN nanowire solar cell. Blue: gallium atoms; Purple: nitrogen atoms; White: hydrogen atoms. Band structures of infinite long (b) p-doped and (c) n-doped GaN nanowires calculated with DFTB method. The black dotted lines mark the Fermi levels.

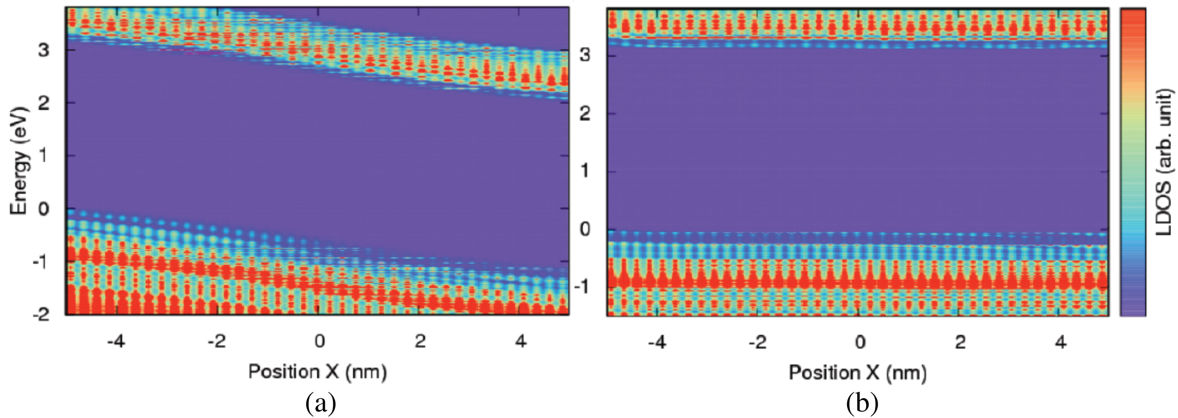

Figure 2. Local density of states of GaN nanowire. $X < 0$ nm corresponds to p-doped region while $X > 0$ nm corresponds to n-doped region.

is established when the p-n junction is formed. The optical excitation and charge transport processes in nanoscale devices depend strongly on the electronic structure of the system. Figs. 2(a) and (b) plot the local density of states (LDOS) of the nanowire under 2.0 V and 3.1 V forward bias voltage, respectively. The energy levels distribution along wire axis is shown. The left region of nanowire is p-doped while the right region is n-doped. The underlying mechanism for the coupled optical-electrical processes is as follow: (1) electron-hole pairs are generated in the device upon light illumination. (2) Electrons are drifted by the V_{bi} and flow from p-type to n-type region while hole flows in the opposite direction. (3) Charge carriers are collected at two ends, giving rise to photocurrent. Under forward bias voltages, the potential barrier at the junction is reduced. Fig. 2(b) shows the LDOS with applied bias voltage of 3.1 V where the device approaches flat-band condition. The charge carriers can then move in opposite directions driven by the applied voltage. At open-circuit voltage, the charge carriers experience a balance of the two counteracting forces, and no net current is observed.

Next, we investigate the electrical characteristics of the nanowire device by varying the bias potential at the electrical contacts of the solar cell. The I-V curve of the GaN nanowire is shown in Fig. 3. The black lines represent the dark currents while the red lines plot the total currents under

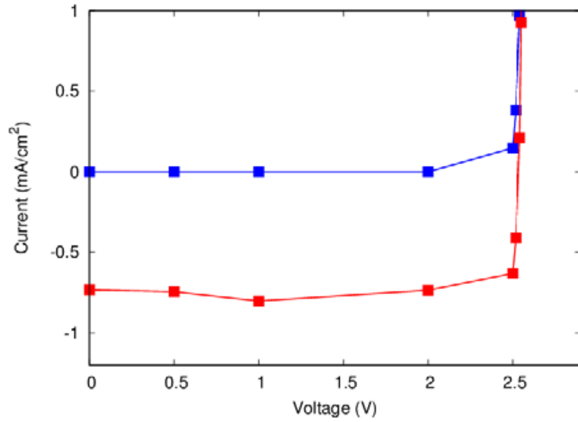

Figure 3. *I*-*V* curves of the GaN nanowire with and without light illumination. Monochromatic light is chosen with photon energy set as 3.3 eV. Incident light power is $1\,\mathrm{kW/m^2}$. Blue line shows the dark current and red line shows the total current.

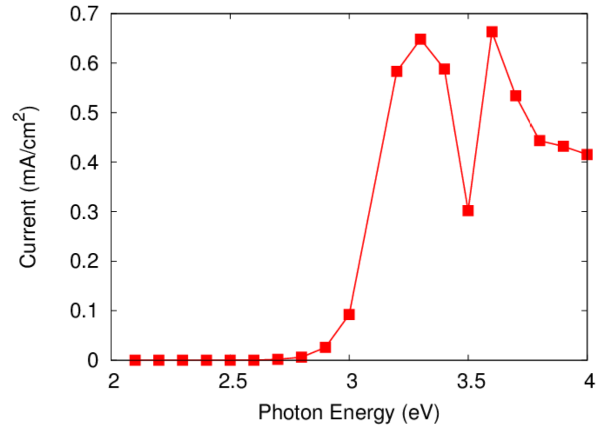

Figure 4. Short-circuit current versus photon energy for GaN nanowire under monochromatic light illumination with incident light power of $1\,\mathrm{kW/m^2}$.

monochromatic light illumination. The photon energy is set as 3.3 eV. In dark, the GaN nanowire shows the electrical characteristics of a diode. With increasing bias voltage, the injection barrier is reduced, and current starts to flow after a threshold voltage. Under illumination, photons are absorbed and give rise to photocurrent without external bias voltage. From Fig. 3, the short-circuit current of the GaN nanowire is $0.73\,\mathrm{mA/cm^2}$, and the open-circuit voltage is 2.52 V.

Figure 4 plots the short-circuit currents with respect to photon energy. We note that at low photon frequencies, no photocurrent is generated in the device due to the wide band gap of GaN. The photon does not have enough energy to generate electron-hole pair. The device shows an onset of current at photon energy of about 3 eV, and the current increases substantially as the photon energy approaches the band gap of the nanowire. When the photon energy is larger than the band gap, electrons are excited from valence band to conduction band. Eventually, the electron-hole pair migrates and separates at the *p*-*n* junction. The reduced photocurrent at 3.5 eV is attributed to the narrow conduction band of Ga 4*p* orbitals where a low density of states is found. Compared to Si nanowire [12], GaN nanowire shows photoresponse at higher energies in near-UV range of solar spectrum. The results suggest that an accurate description of electronic structures is crucial for studying performance of nanoscale devices. In addition, atomistic modeling is increasingly important due to the continuous miniaturization of technology and diversification of device architectures.

4. SUMMARY

A quantum mechanical approach for modeling coupled optical electrical processes in nanoscale devices is presented. By including proper self-energies electron reservoirs and electromagnetic field, the photoresponse of the devices open to electron reservoirs under bias can be described. The current approach is useful not only for modeling optical excitation and relaxation processes in nanoscale devices, but also for understanding the mechanism of energy conversion and improving the design of next generation optoelectronic devices. We demonstrate the method by numerical study of the coupled optical electrical processes in GaN nanowire solar cells. The results show that performance of the device depends crucially on electronic structures. Strong photoresponse of GaN devices is found near the UV region of the solar spectrum due to wide band gap of GaN. To enhance the power conversion efficiency of devices, band gap engineering of GaN nanowires has been proposed by surface functionalization and strain effects [24, 25]. In addition, metallic nanoparticles that support plasmonic effects can be exploited for light trapping to improve light absorption [15].

ACKNOWLEDGMENT

The financial support from the National Natural Science Foundation of China (21322306(C.Y.Y.), 21273186(G.H.C., C.Y.Y.)), National Basic Research Program of China (No. 2014CB921402 (C.Y.Y.)), and University Grant Council (AoE/P-04/08(G.H.C., C.Y.Y.)) is gratefully acknowledged.

REFERENCES

1. Meng, L. Y., Y. Shang, Q. K. Li, Y. F. Li, X. W. Zhan, Z. G. Shuai, R. G. E. Kimber, and A. B. Walker, "Dynamic Monte Carlo simulation for highly efficient polymer blend photovoltaics," *J. Phys. Chem. B*, Vol. 114, No. 1, 36–41, 2010.
2. Koster, L. J. A., E. C. P. Smits, V. D. Mihailetchi, and P. W. M. Blom, "Device model for the operation of Polymer/fullerene bulk heterojunction solar cells," *Phys. Rev. B*, Vol. 72, No. 8, 085205, 2005.
3. Keldysh, L.-V., "Diagram technique for nonequilibrium processes," *Sov. Phys. JETP*, Vol. 20, 1018, 1965.
4. Meir, Y. and N. S. Wingreen, "Landauer formula for the current through an interacting electron region," *Phys. Rev. Lett.*, Vol. 68, 2512, 1992.
5. Jauho, A.-P., N. S. Wingreen, and Y. Meir, "Time-dependent transport in interacting and noninteracting resonant-tunneling systems," *Phys. Rev. B*, Vol. 50, No. 8, 5528, 1994.
6. Zheng, X., F. Wang, C. Y. Yam, Y. Mo, and G. H. Chen, "Time-dependent density-functional theory for open systems," *Phys. Rev. B*, Vol. 75, No. 19, 195127, 2007.
7. Kwok, Y. H., H. Xie, C. Y. Yam, X. Zheng, and G. H. Chen, "Time-dependent density functional theory quantum transport simulation in non-orthogonal basis," *J. Chem. Phys.*, Vol. 139, No. 22, 224111, 2013.
8. Wang, R. L., X. Zheng, Y. H. Kwok, H. Xie, G. H. Chen, and C. Y. Yam, "Time-dependent density functional theory for open systems with a positivity-preserving decomposition scheme for environment spectral functions," *J. Chem. Phys.*, Vol. 142, No. 14, 144112, 2015.
9. Henrickson, L. E., "Nonequilibrium photocurrent modeling in resonant tunneling photodetectors," *J. Appl. Phys.* , Vol. 91, No. 10, 6273–6281, 2002.
10. Galperin, M. and A. Nitzan, "Current-induced light emission and light-induced current in molecular-tunneling junctions," *Phys. Rev. Lett.*, Vol. 95, 206802, 2005.
11. Galperin, M. and A. Nitzan, "Molecular optoelectronics: The interaction of molecular conduction junctions with light," *Phys. Chem.*, Vol. 14, 9421, 2012.
12. Zhang, Y., L. Y. Meng, C. Y. Yam, and G. H. Chen, "Quantum-mechanical prediction of nanoscale photovoltaics," *J. Phys. Chem. Lett.*, Vol. 5, 1272, 2014.
13. Fetter, A. L. and J. D. Walecka, *Quantum Theory of Many Particle Systems*, Dover, New York, 1971.
14. Yam, C. Y., L. Y. Meng, Y. Zhang, and G. H. Chen, "A multiscale quantum mechanics/electromagnetics method for device," *Chem. Soc. Rev.*, Vol. 44, 1763, 2015.
15. Meng, L. Y., C. Y. Yam, Y. Zhang, R. L. Wang, and G. H. Chen, "Multiscale modeling of plasmon-enhanced power conversion efficiency in nanostructured solar cells," *J. Phys. Chem. Lett.*, Vol. 6, 4410, 2015.
16. Porezag, D., T. Frauenheim, T. Köhler, G. Seifert, and R. Kaschner, "Construction of tight-binding-like potentials on the basis of density-functional theory: Application to carbon," *Phys. Rev. B*, Vol. 51, No. 19, 12947, 1995.
17. Elstner, M., D. Porezag, G. Jungnickel, J. Elsner, M. Haugk, T. Frauenheim, S. Suhai, and G. Seifert, "self-consistent-charge density-functional tight-binding method for simulations of complex materials properties," *Phys. Rev. B*, Vol. 58, No. 11, 7260, 1998.
18. Pearton, S. J. and F. Ren, "GaN electronics advanced materials," *Adv. Mater.*, Vol. 12, 1571, 2000.

19. Shui, R. J., G. A. Vawter, C. G. Willison, M. M. Bridges, J. W. Lee, S. J. Pearton, and C. R. Abernathy, "Comparison of plasma etch techniques for III-V nitrides," *Solid State Electron.*, Vol. 42, 2259, 1998.
20. Johnson, J. C., et al., "Single gallium nitride nanowire lasers," *Nat. Mater.*, Vol. 1, 106, 2002.
21. Wallentin, J., et al., "InP nanowire array solar cells achieving 13.8% efficiency by exceeding the ray optics limit," *Science*, Vol. 339, 1057–1060, 2013.
22. Krogstrup, P., et al., "Single-nanowire solar cells beyond the Shockley-Queisser limit," *Nat. Photon.*, Vol. 6, 306–310, 2013.
23. Ramer, N. J. and A. M. Rappe, "Virtual-crystal approximation that works: Locating a compositional phase boundary in $Pb(Zr_{1-x}Ti_x)O_3$," *Phys. Rev. B*, Vol. 62, R743, 2000.
24. Carter, D. J., J. D. Gale, B. Delley, and C. Stampfl, "Geometry and diameter dependence of the electronic and physical properties of GaN nanowires from first principles," *Phys. Rev. B*, Vol. 77, 115349, 2008.
25. Fang, D. Q., A. L. Rosa, Th. Frauenheim, and R. Q. Zhang, "Band gap engineering of GaN nanowires by surface functionalization," *Appl. Phys. Lett.*, Vol. 94, 073116, 2009.